

SCIENTIFIC REPORTS



OPEN

Proteomic and Carbonylation Profile Analysis at the Critical Node of Seed Ageing in *Oryza sativa*

Guangkun Yin^{1,*}, Xia Xin^{1,*}, Shenzao Fu^{1,2,*}, Mengni An¹, Shuhua Wu¹, Xiaoling Chen¹, Jinmei Zhang¹, Juanjuan He¹, James Whelan³ & Xinxiong Lu¹

Received: 16 September 2016

Accepted: 07 December 2016

Published: 17 January 2017

The critical node (CN), which is the transition from the plateau phase to the rapid decreasing phase of seed ageing, is extremely important for seed conservation. Although numerous studies have investigated the oxidative stress during seed ageing, information on the changes in protein abundance at the CN is limited. In this study, we aimed to investigate the abundance and carbonylation patterns of proteins at the CN of seed ageing in rice. The results showed that the germination rate of seeds decreased by less than 20% at the CN; however, the abundance of 112 proteins and the carbonylation levels of 68 proteins markedly changed, indicating oxidative damage. The abundance and activity of mitochondrial, glycolytic, and pentose phosphate pathway proteins were reduced; consequently, this negatively affected energy production and germination. Proteins related to defense, including antioxidant system and heat shock proteins, also reduced in abundance. Overall, energy metabolism was reduced at the CN, leading to a decrease in the antioxidant capacity, whereas seed storage proteins were up-regulated and carbonylated, indicating that the seed had a lower ability to utilize seed storage proteins for germination. Thus, the significant decrease in metabolic activities at the CN might accelerate the loss of seed viability.

A notable characteristic of seed viability is the reverse S-shaped survival curve during ageing, which includes a plateau phase (Phase I; P-I), followed by a rapid decreasing phase (Phase II; P-II) and a slow decreasing phase (Phase III; P-III). The transformation from P-I to P-II is defined as the critical node (CN), which is highly important for seed conservation¹. The average germination of approximately 42,000 diverse accessions stored for 16 to 81 years at the National Center for Genetic Resources Preservation, USA has been decreased by 42%². The average germination rate of peanut (stored for 34 years), soybean (stored for 36 years), wheat (stored for 43.6 years), and barley (stored for 44.4 years) is 6%, 21%, 73%, and 86%, respectively³. Similar results have been also reported by the Genebank of the Leibniz Institute of Plant Genetics and Crop Plant Research (IPK), Germany⁴. Rice is extremely important food crop. One of main aims in genebanks is maintaining the rice seed safe conservation. At the T.T. Chang Genetic Resources Center in International Rice Research Institute, 183 rice accessions stored up to 30 years showed more than 70% germination⁵, and more than 93% of seed lots produced in 1980 still maintained 85% germination after 33 years in storage⁶. Owing to the reduction in seed viability, the regeneration of genetic resources is considered crucial for maintaining genetic integrity. Previous studies have shown that seed regeneration needs to be carried out prior to the CN in order to prevent a large decrease in viability, which can lead to changes in genetic composition^{7,8}. Previously, we showed that the mitochondrial ultrastructure of seed at the CN is abnormal owing to the decreased oxygen consumption as well as the decreased activity of cytochrome *c* oxidase and malate dehydrogenase (MDH)¹.

The role of reactive oxygen species (ROS) in the loss of seed viability has been well investigated. During natural or accelerated ageing, the levels of seed antioxidative enzymes (e.g., superoxide dismutase, SOD; catalase, CAT; ascorbate peroxidase, APX; and glutathione reductase, GR) and antioxidants (ascorbic acid and glutathione) decrease, leading to the accumulation of ROS and consequently oxidative damage^{9,10}. The proteomic analysis of aged maize seeds indicated that the loss of seed viability loss is related to ROS damage¹¹. The reduction

¹National Genebank, Institute of Crop Science, Chinese Academy of Agricultural Sciences, Beijing 100081, China.

²China National Rice Research Institute, Hangzhou 310006, China. ³Australian Research Council Centre of Excellence in Plant Energy Biology, School of Life Science, La Trobe University, Bundoora, Victoria 3083, Australia. ⁴These authors contributed equally to this work. Correspondence and requests for materials should be addressed to J.W. (email: J.W.whelan@LaTrobe.edu.au) or X.L. (email: luxinxiong@caas.cn)

in antioxidant capacity, i.e., decrease in the expression of *CAT1*, *APX1*, and *MDHAR1* may be responsible for the loss of rice seed viability during storage¹². The mitochondrial structure and function alter in aged seeds. For instance, in aged soybean seeds, the mitochondrial ascorbic acid and glutathione cycle activity decreased, leading to elevated ROS accumulation¹³. The aged seed induces dynamic changes in mitochondrial physiology via the increased ROS production, resulting in an irreversible loss of seed viability¹⁴. Seed possess many repair enzymes, such as PROTEIN L-ISOASPARTYL O-METHYLTRANSFERASE, for preventing age-induced ROS accumulation to improve seed vigor and longevity¹⁵.

ROS accumulation can induce the formation of protein carbonyls that affect enzyme activity and lead to ageing or death^{16,17}. Numerous studies have reported that protein carbonylation contributes to leaf and fruit senescence as well as the decreased rate of seed germination^{18–20}. In *Arabidopsis*, HSP70 and LEA were carbonylated after ageing treatment²¹, whereas seed storage proteins (SSPs) were carbonylated during storage²². In this study, we aimed to determine the changes in protein abundance and protein carbonylation at the CN of seed ageing in rice. The carbonylated protein patterns were analyzed by two-dimensional (2D) gel electrophoresis followed by western blotting with antidinitrophenyl hydrazine (DNP) antibodies. The carbonylation level and pattern of several proteins might be indicators of seed ageing, and could help to improve seed storage management.

Results

Proteomic and carbonylation profile analysis at the CN. In our previous study, rice seed vigor loss displayed a P-I, and then experienced a rapid decreasing phase after 84% germination (P-II). Therefore, we chose the seed germination percentage at 84% as the critical node¹. Seed vigor was analyzed from maximum to the CN, as it is this stage that is extremely important for safe conservation of seeds in genebank. This differed to previous studies in *Arabidopsis*²¹, maize¹¹, and *Brassica napus* seeds²³ where comparison was made at the end of Phase II.

Proteomic and carbonylation profile analysis was carried out to determine the impact of oxidative stress at the CN. Protein profiles of rice embryos was extracted from 97% (control), 92% and 84% germination percentage after 0 d, 3 d, and 4 d aged treatment, respectively, and separated by gel electrophoresis using immobilized pH gradient (IPG) strips in isoelectric focusing (IEF). Three biological repeats were used for either gels or blots of each sample. More than 700 protein spots were detected on 12% (v/v) sodium dodecyl sulfate polyacrylamide gel electrophoresis (SDS-PAGE) gels by PDQuest 8.0 (Fig. 1). The abundance of 112 protein spots showed a change higher than 1.5-fold at the CN which MOWSE score were higher than 65 (Table 1). Of them, 78 downregulated proteins (D1–D78) and 17 upregulated proteins (U1–U17) were identified in all treated seeds; 11 upregulated proteins (U18–U28) were uniquely detected in 3-d aged seeds; and six upregulated proteins (U29–U34) were uniquely detected in 4-d aged seeds (Tables 1 and 2). Figure 2 shows the change pattern of different proteins related to energy, defense, metabolism, growth or division, transcription, and other unknown functions²⁴.

To better understand protein carbonylation at the CN, we performed in-strip derivatization with 2,4-dinitrophenylhydrazine (DNPH) followed by SDS-PAGE and immunochemical detection of carbonylated proteins. Figure 3 shows carbonylated proteins from rice seeds in 2D blots. The level of carbonylated proteins on the polyvinylidene difluoride (PVDF) membrane was normalized to the protein level of the corresponding protein spot on 2D gels, and only reproducible differences were considered to be changes. The results showed that 32 (C1–C32) out of 78 downregulated proteins and 8 out of 36 upregulated proteins (C33–C40) displayed significant carbonylation. Additionally, 11 upregulated proteins (C41–C51) and 17 downregulated proteins (C52–C68) showed no significant change in abundance on 2D gels, but displayed significant changes in carbonylation (Table 3). Overall, seed proteins underwent carbonylation at the CN.

Downregulated proteins at the CN. The 78 downregulated proteins were related to energy (29%), defense (21%), metabolism (14%), protein synthesis (8%), protein destination and storage (6%), transcription (5%), growth or division (4%), secondary metabolism (3%), transporting (1%), signal transduction (1%), and other unknown functions (2%) (Fig. 2A). Additionally, carbonylation was observed among those proteins at the CN, further suggesting that the related functions could be disrupted.

Proteins related to energy metabolism. A total of 16 downregulated proteins were related to energy metabolism (Table 1). The β -ATP synthase subunit (β ATP), MDH, and succinate dehydrogenase (SDH) showed decrease in abundance (D14, D19, and D48) and significant carbonylation (C12, C16, and C27) (Table 1). To better understand protein expression at the CN, the activity of MDH was measured in aged seeds after imbibition for 48 h. As compared to the control, the activity of MDH showed a decrease by 11% and 20% in 3-d and 4-d aged seeds, respectively (Fig. 4A), which was consistent with the decrease in abundance. *MDH1* also displayed a steady downregulation with ageing (Fig. 5A). Compared with the control, *SDH1* showed a decrease by 16% and 40% in 3-d and 4-d aged seeds, respectively (Fig. 5B). The immunodetection of the β ATP subunit showed a significant decrease at the CN (Fig. 5G). Compared with the control, β ATP showed a decrease by 25% and 45% in 3-d and 4-d aged seeds, respectively (Fig. 5C). These results indicated that mitochondrial metabolism significantly decreased at the CN.

Seven proteins of the glycolytic pathway, including phosphoglycerate mutase (D4), pyruvate decarboxylase (PDC, D8), triosephosphate isomerase (D29 and D53), D-glyceraldehyde 3-phosphate enolase (D58 and D63), and pyrophosphate-dependent phosphofructokinase (D62) were downregulated, indicating that glycolytic metabolism was also reduced at the CN. Of these proteins, D4, D8, D29, and D63 also showed significant carbonylation (C4, C7, C30 and C31) (Table 1). Compared with the control, the activity of PDC showed a decrease by 23% and 30% in 3-d and 4-d aged seeds, respectively (Fig. 4B). In this study, *PDC1* did not show any significant change at the CN (Fig. 5D). Additionally, 6-phosphogluconate dehydrogenase (6PGD, D7) of the oxidative pentose phosphate pathway (PPP) showed a decrease in abundance and significant carbonylation (C6). Compared

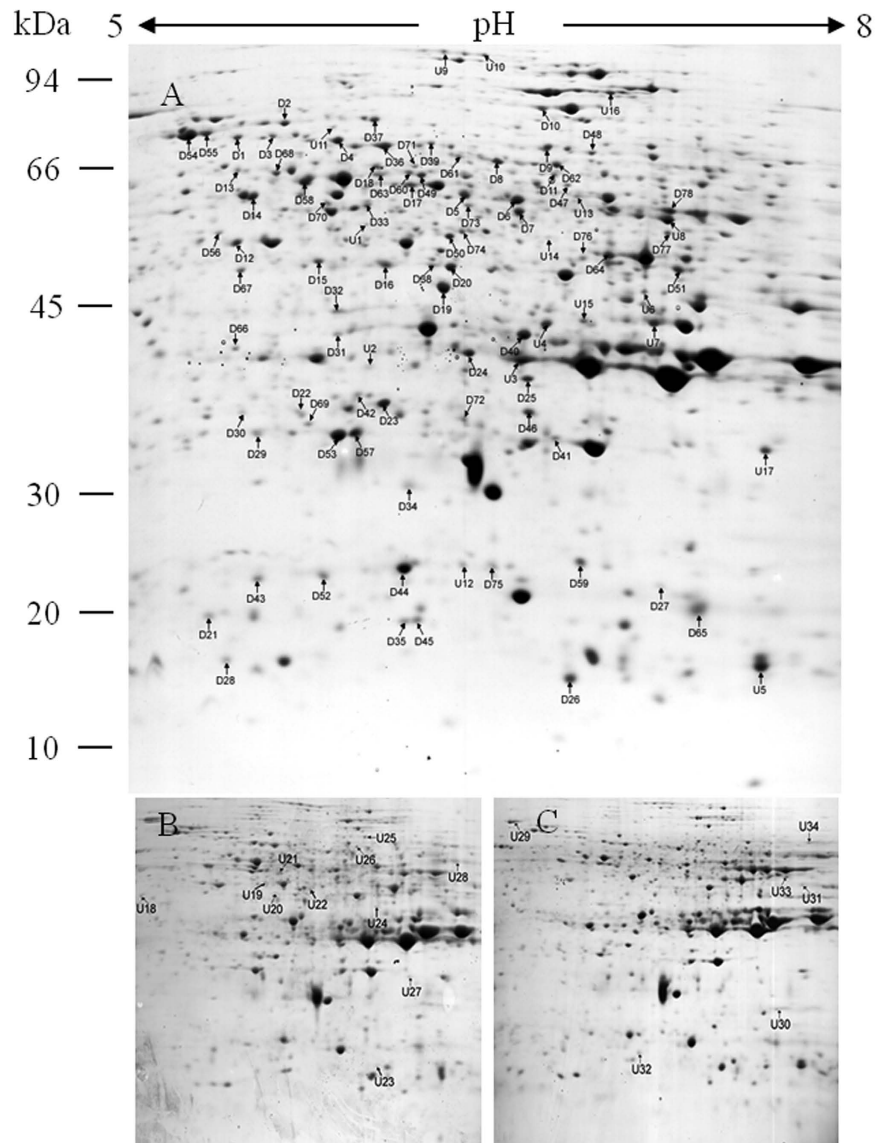


Figure 1. Representative isoelectric focusing (IEF)/dodecyl sulfate polyacrylamide gel electrophoresis (SDS-PAGE) separation gels of proteins from 0 d (A), 3 d (B) and 4 d (C) aged rice seeds after imbibition for 48 h. Total 500 μ g protein were separated by immobilized pH gradient (IPG) strips and 12% (w/v) SDS-PAGE gels. Protein codes correspond to those in Tables 1, 2 and 3. Number on the left represents the apparent molecular mass. Number above the gels represents the pI of separated protein spot. U, upregulation; D, downregulation.

with the control, the activity of 6PGD showed a decrease by 15% and 33% in 3-d and 4-d aged seeds, respectively, whereas 6PGD1 showed a decrease by 37% and 56%, respectively (Figs 4C and 5E). These results indicated that PPP was significantly inhibited at the CN.

Proteins related to defense. In this study, 12 downregulated proteins were related to defense, indicating the decreased ability of aged seeds to combat oxidative stress. Compared with the control, the activity of ascorbate peroxidase 1 (APX, D57) decreased by 47% and 33% in 3-d and 4-d aged seeds, respectively (Fig. 4D). APX1 showed a steady decrease with ageing (Fig. 5F). Additionally, the reduced abundance in cytosolic APX proteins at the CN was confirmed by immunodetection using the cytosolic APX antibody (Fig. 5G) and indicated ROS accumulation at the CN of seed ageing. Compared with the control, the activity of glutathione S-transferase (GST, D46) decreased by 87% and 70% in 3-d and 4-d aged seeds, respectively (Fig. 4E), negatively affecting the ability of the antioxidant defense system. GST showed a decrease in abundance and significant carbonylation (C26). Five heat shock proteins (HSPs), including HSP70 (D2, D54, and D55), 17.9-kDa class I HSP (D13), 18.0-kDa class II HSP (D44), and two chaperonins (D13 and D60) significantly downregulated at the CN, whereas the HSP D2 and D44 and the chaperonin D13 showed significant carbonylation (C2, C25 and C11).

Spot	Protein name	Accession No.	Scores	Fold		Carbonylation
				0d/3d	0d/4d	
Energy						
D1	Vacuolar proton-ATPase	NP_001058280.1	890	1.85	4.54	C1
D4	Phosphoglycerate mutase	NP_001044625.1	1094	1.59	2.74	C4
D5	ATP synthase lipid-binding protein	YP_002000594.1	773	1.82	2.55	C5
D6	ATP synthase lipid-binding protein	YP_002000594.1	744	1.71	3.01	
D7	6-phosphogluconate dehydrogenase 1	NC_029261.1	1067	2.93	5.99	C6
D8	Pyruvate decarboxylase	BAC20138.1	446	1.49	2.29	C7
D14	ATP synthase subunit beta	NP_001043900.1	1482	1.59	2.11	C12
D19	Malate dehydrogenase	NP_001064860.1	903	1.35	30.02	C16
D22	Cyt-RPEase	NP_001063604.2	187	1.93	5.13	
D29	Triosephosphate isomerase	AAB63603.1	689	1.29	3.06	
D30	Carboxymethylenebutenolidase-like protein	NP_001043244.1	536	1.16	1.42	
D36	Pyruvate decarboxylase 2	NP_001049811.1	615	1.18	2.17	C21
D48	Succinate dehydrogenase flavoprotein subunit	NP_001058845.1	123	1.26	1.82	C27
D53	Triosephosphate isomerase	AAB63603.1	995	1.26	2.44	C30
D58	Enolase	AAC49173.1	1075	1.79	1.98	C31
D61	Pyruvate decarboxylase 1	NC_029260.1	147	1.19	2.39	
D62	Phosphofructokinase beta subunit	NP_001057284.1	596	1.04	2.66	
D63	Beta-enolase	AAC49173.1	269	2.34	1.48	
D64	ADH1	ADH03842.1	997	2.36	1.87	C32
D69	Vacuolar ATP synthase 16kDa proteolipid subunit	AAO72561.1	145	∞	∞	
D70	Ketol-acid reductoisomerase	NP_001043738.1	186	∞	∞	
D74	UDP-glucose 6-dehydrogenase 3	NP_001051328.1	568	∞	∞	
D78	Glyceraldehyde-3-phosphate dehydrogenase 2,	NP_001053139.1	451	∞	∞	
disease/defense						
D2	70 kDa heat shock protein	ABF95267.1	502	1.51	2.33	C2
D13	Chaperonin CPN60-1, mitochondrial	NP_001048938.1	248	2.40	3.24	C11
D26	Dehydration stress-induced protein	NP_001064434.1	192	1.49	2.58	
D38	Salt tolerance protein 5	NP_001057221.1	153	1.16	4.14	C23
D44	17.9kDa class I heat shock protein	NP_001049657.1	686	1.06	1.51	C25
D46	Glutathione S-transferase 2	NP_001044339.1	282	1.39	2.46	C26
D52	18.0kDa class II heat shock protein	NP_001042231.1	339	1.17	1.88	
D54	70 kDa heat shock protein	ABA95501.2	813	1.49	2.55	
D55	70 kDa heat shock protein	NP_001044757.1	725	1.46	2.42	
D56	Silver leaf whitefly-induced protein 1	NP_001047794.1	653	1.38	1.50	
D57	L-ascorbate peroxidase 1	NP_001049769.1	639	3.32	10.89	
D59	Cold shock domain protein 2	NP_001060914.1	525	1.91	1.94	
D60	TCP-1/cpn60 chaperonin	AAT77033.1	338	1.28	1.82	
D72	Germin-like protein 8-2	AAC04834.1	136	∞	∞	
D73	GDP-mannose 3,5-epimerase 2	NP_001068183.1	290	∞	∞	
D75	Germin-like protein 8-2	AAC04834.1	106	∞	∞	
Metabolism						
D10	5-methyltetrahydropteroyltriglutamate-homocysteine methyltransferase	ABG22095.1	1087	2.89	4.92	C9
D15	Glutamine synthetase cytosolic isozyme 1-1	NP_001048045.1	328	1.88	3.78	C13
D16	Reversibly glycosylated polypeptide	CAA77235.1	178	1.63	9.04	
D17	Methylmalonate semi-aldehyde dehydrogenase	NP_001059082.1	412	2.23	4.65	C14
D18	Ketol-acid reductoisomerase	NP_001043738.1	663	1.50	4.47	C15
D20	Reversibly glycosylated polypeptide	CAA77235.1	906	1.53	2.93	C17
D37	Phosphoglucomutase	NP_001051066.1	470	1.09	6.36	C22
D41	Proteasome subunit beta type-1	NP_001063603.1	663	1.18	2.33	
D47	Inosine-5'-monophosphate dehydrogenase 1	AAK09225.1	598	1.17	1.94	
D49	Leucyl-cystinyl aminopeptidase	Q6K669.1	1325	1.37	3.83	C28
D50	S-adenosylmethionine synthase	P93438.1	638	1.61	2.21	
protein synthesis						
D32	60 S acidic ribosomal protein P0	NP_001060923.1	531	1.09	2.49	C19
D40	Guanine nucleotide-binding protein subunit beta	NP_001043910.1	1053	1.25	1.40	
Continued						

Spot	Protein name	Accession No.	Scores	Fold		Carbonylation
				0d/3d	0d/4d	
D65	Bowman Birk trypsin inhibitor	BAD52869.1	107	1.37	1.52	
D67	Succinyl-CoA ligase [ADP-forming] subunit beta	NP_001047463.1	145	∞	∞	
D68	Mitochondrial processing peptidase beta subunit	NP_001049357.1	194	∞	∞	
D76	Mitochondrial import inner membrane translocase subunit Tim17/Tim22/Tim23 family protein	NP_001049884.1	106	∞	∞	
protein destination and storage						
D28	Cupin family protein	AAS07324.1	394	1.66	2.97	
D42	Cupin family protein	ABF95817.1	202	1.21	2.92	
D43	Cupin family protein	ABF95817.1	376	1.31	1.68	
D71	Cupin family protein	ABF95817.1	236	∞	∞	
D77	Cupin family protein	ABF95817.1	144	∞	∞	
Transcription						
D21	Elicitor-inducible protein EIG-J7	NP_001048145.1	232	1.52	5.34	
D35	Glycine-rich RNA-binding protein 7	AAT85299.1	464	1.29	3.72	
D39	Asparagine-tRNA ligase	NP_001043066.1	460	1.14	2.74	C24
D45	Glycine-rich RNA-binding protein GRP1A	NP_001067344.1	64	1.49	1.66	
growth/division						
D12	Actin	BAB63635.1	700	1.43	3.82	C10
D51	Late embryogenesis abundant protein 1	A2XG55.2	355	1.21	1.35	C29
D66	Spermidine synthase 1	NP_001059438.1	183	∞	∞	
secondary metabolism						
D31	NADH-dependent enoyl-ACP reductase	NP_001061557.1	570	1.31	6.18	
D34	Lactoylglutathione lyase	NP_001055113.1	186	1.14	4.01	
Transporters						
D9	ECF transporter A component EcfA	BAD11555.1	777	1.72	3.95	C8
signal transduction						
D33	GDP dissociation inhibitor	NP_001055566.1	550	1.71	2.61	C20
unclear classification						
D3	Os09g0491772 protein	NP_001175918.1	241	1.54	2.91	C3
D11	OSJNBa0010H02.6 protein	NP_001053500.1	748	1.67	3.05	
D23	Uncharacterized protein	NP_001056364.1	803	1.32	1.90	
D24	OSJNBa0004N05.4 protein	CAE03380.1	608	1.42	2.44	C18
D25	Uncharacterized protein P0435H01.4	NP_001044131.1	654	1.53	2.07	
D27	Uncharacterized protein P0036D10.5	NP_001174164.1	238	1.46	2.57	

Table 1. Proteins with significantly decreased abundance at the critical node in 0-d, 3-d, and 4-d aged rice seeds. Mascot scores >65 are statistically significant at $p < 0.05$.

Upregulated proteins at the CN. Compared with the control, 31 upregulated proteins were related to storage, energy, disease and defense, metabolism, protein synthesis, growth and division, and other unknown functions (Fig. 2B). SSPs formed the largest group of upregulated proteins that included globuline, glutelin, and cupin (Table 2), which showed various experimental molecular weights, indicating that SSPs were post-translationally modified or broken down (Fig. 3). In this study, we also identified 17 SSPs that displayed significant carbonylation, of which 10 were upregulated, whereas the rest showed no change in abundance (Tables 2 and 3).

Discussion

The viability of aged seeds is an important aspect for maintaining genetic diversity during seed storage. In this study, we demonstrated the occurrence of oxidative damage that primarily affects the abundance of proteins related to energy generation, metabolism, and defense. These findings were in agreement with previous studies in *Arabidopsis*, which showed that proteins related to energy, metabolism, and defense play key roles in seed maintenance and are downregulated at the CN^{21,22}. The changes occurring in protein abundance appeared to be related to oxidative stress^{25,26}, resulting in an inability to utilize seed storage proteins, as the latter increased in abundance at the CN.

Proteins related to energy metabolism formed the largest group of downregulated proteins (Fig. 2A). The capacity of energy supply is highly important for seed germination and seedling growth, since large amounts of energy are needed prior to the establishment of photosynthesis in the plant²⁷. Previous studies in *Arabidopsis* reported that one of the earliest events during germination is the upregulation of approximately 600 genes that encode proteins related to mitochondrial functions and are critical for germination^{28,29}. A variety of mitochondrial mutants involved in electron transport showed slow germination rates or high seedling lethality²⁸. The downregulated proteins of mitochondria were observed by carbonylated modification, including β ATP, MDH

Spot	Protein name	Accession No.	Scores	Fold		Carbonylation
				3d/0d	4d/0d	
protein destination and storage						
U14	Glutelin type-A 2	BAC77349.1	362	1.41	2.20	C39
U3	Cupin family protein	NP_001051533.1	554	1.01	2.35	C34
U4	Cupin family protein	NP_001051533.1	438	1.74	4.09	
U15	Globulin-like protein	AAM33459.2	472	1.63	1.67	
U5	Glutelin	NP_001046769.1	205	1.32	3.22	
U11	Glutelin type-A 2	CAA38211.1	274	1.83	2.81	
U8	Vicilin storage protein	AAM33459.2	479	2.42	4.04	
U18	Cupin family protein	NP_001051533.1	511	∞	0	
U27	Cupin family protein	NP_001173574.1	198	∞	0	
U28	Cupin family protein	BAC77349.1	425	∞	0	
U32	Globulin-like protein	AAM33459.2	371	0	∞	
energy						
U1	Pullulanase	ACY56106.1	161	1.95	3.18	
U9	H0806H05.4 protein	CAC09471.2	542	1.42	2.62	C35
U10	H0806H05.4 protein	CAC09471.2	312	3.31	5.48	C36
U12	1,4-alpha-glucan-branching enzyme	BAA01584.1	115	1.14	1.98	C37
U21	ATP-citrate synthase alpha chain protein	NP_001067052.1	196	∞	0	
U29	Peroxisiredoxin-2C	NP_001043845.1	276	0	∞	
U30	Peroxisiredoxin-2C	NP_001043845.1	509	0	∞	
U34	Nucleoside diphosphate kinase	NP_001065404.1	246	0	∞	
disease/defense						
U2	Heat shock protein 90-1	BAD04054.1	205	1.56	2.16	C33
U6	ABA-responsive protein	ABA98234.1	156	1.68	3.26	
U22	GDP-mannose 3,5-epimerase 2	NP_001068183.1	195	∞	0	
U23	Dehydration stress-induced protein	NP_001057177.1	170	∞	0	
signal transduction						
U13	Adenosine kinase	BAC02723.1	169	1.39	1.79	C38
U17	GTP-binding nuclear protein Ran-2	NP_001056390.1	553	2.06	2.86	C40
metabolism						
U16	Sucrose synthase 1	NP_001050319.1	103	2.21	3.56	
growth/division						
U19	Meiotic recombination protein SPO11-1	NP_001067760.1	101	∞	0	
Unclear classification						
U7	Os03g0327600 protein	NP_001049995.1	470	1.60	2.16	
U20	OSJNBa0044M19.9 protein	NP_001052622.1	150	∞	0	
U31	Os05g0468800 protein	NP_001055802.2	409	0	∞	

Table 2. Proteins with significantly increased abundance at the critical node in 0-d, 3-d, and 4-d aged rice seeds. Mascot scores >65 are statistically significant at $p < 0.05$.

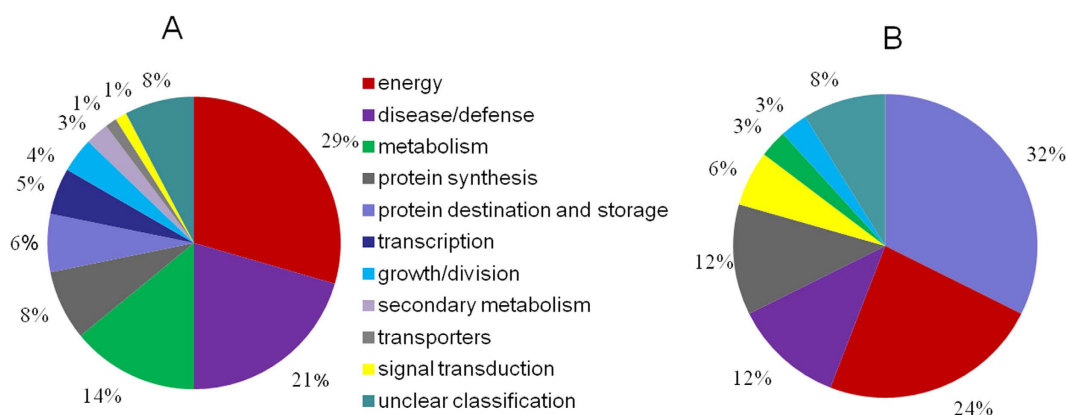


Figure 2. Classification of downregulated (A) and upregulated (B) proteins in 0 d, 3 d, and 4 d aged rice seeds after imbibition for 48 h.

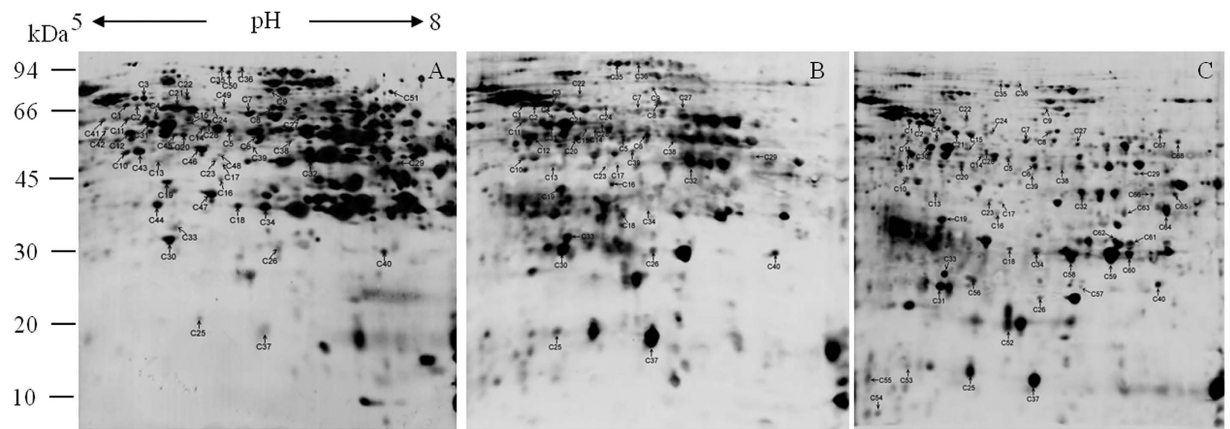


Figure 3. Two-dimensional (2D) immunoblots using antidinitrophenyl hydrazone antibody to detect carbonylated embryo proteins in 0-d (A), 3-d (B), and 4-d (C) aged rice seeds after imbibition for 48 h. Total 500 μ g protein were numbered in a preparative 2D electrophoresis gel and excised for MS/MS analysis, corresponding to the proteins in Tables 1, 2 and 3. Number on the left represents the apparent molecular mass. Number above the gels represents the pI of separated protein spot. (C) Carbonylated spot.

and SDH, respectively (Table 1). Mitochondria plays key roles for energy supplying during seed imbibitions. β ATP is the F_0 sector of ATPase³⁰. The state and function of ATP synthase machinery may determine the energy supplying. β ATP protein and β ATP expression level was significant downregulated at the CN (Fig. 5C,G). Our results were consistent with our previous reported in purified mitochondria from the CN of rice seed ageing¹ that ATP synthase machinery was inactive which leads the ATP supplying was inhibited at the CN. The seed of MDH1 and MDH2 double knockout *Arabidopsis* mutants had a lower content of 2-oxoglutarate during imbibition³¹. In the present study, the activity of MDH and the levels of *MDH1* were significantly decreased and carbonylated in aged seeds compared with the control (Figs 4A and 5A), indicating that the TCA cycle was inhibited at the CN after seed imbibition. In addition, SDH is a key member of the electron transport chain complex II, which catalyzes the oxidation of succinate to fumarate with the reduction of ubiquinone to ubiquinol and participates in succinate dependent O_2 consumption in the electron transport chain³². SDH1 knockout *Arabidopsis* mutants had a decreased activity of the electron transport chain, but an increased amount of ROS under environmental stress³³. We showed that the level of *SDH1* was significantly decreased and carbonylated at the CN (Fig. 5B); these results were in agreement with our previous findings that succinate dependent O_2 consumption is reduced at the CN¹. The decreased activity of SDH might cause ROS accumulation and oxidative damage. Overall, these results demonstrated that the mitochondrial metabolism was inhibited at the CN, decreasing the production of ATP and its intermediates, which are needed for seed germination and ROS accumulation.

Several proteins whose showed a decrease in proteins abundance and exhibited different carbonylation levels were observed which involved in the glycolytic pathway, including phosphoglycerate mutase which catalyzes the conversion of 3-phosphoglycerate to 2-phosphoglycerate³⁴, pyruvate decarboxylase (PDC) which catalyzes the decarboxylation of pyruvic acid to acetaldehyde and carbon dioxide³⁵, triosephosphate isomerase which catalyzes the reversible interconversion of the triose phosphate isomers dihydroxyacetone phosphate D-glyceraldehyde 3-phosphate³⁶, enolase which catalyzes the conversion of 2-phosphoglycerate to phosphoenolpyruvate³⁷, and pyrophosphate-dependent phosphofructokinase which catalyzes the reversible phosphorylation of fructose-6-phosphate to fructose-1,6-bisphosphate³⁸. Interestingly, PDC gene family was induced in response to environmental stress in plants^{39,40}. By comparison, *PDC1* level showed no significant change in the aged seed (Fig. 5D). We propose that the decrease of the PDC activity (Fig. 4B) caused by carbonylation may result in deleterious downstream pathway of glycolytic metabolism, leading to a reduction of energy supplying. These results indicated that glycolytic metabolism was also reduced at the CN. 6PGD was carbonylated modification and showed downregulation in aged seed, which converts 6-phosphogluconate to ribose-5-phosphate and produces NADPH in oxidative pentose phosphate pathway (PPP)⁴¹. The decrease in the activity and transcript level of 6PGD resulted in reduction of NADPH production, indicating that PPP metabolism was inhibited at the CN. Taken together, the key members of energy supplying were downregulated and carbonylated modification at the CN, which might cause impairment of mitochondrial, glycolysis and PPP metabolism and then lead to decrease in energy supplying during imbibition, in turn, trigger a cascade of deleterious metabolism which could contribute to the process of ageing disorders.

Proteins related to defense were downregulated at the CN (Fig. 2A). APX1 plays an important role in the antioxidative metabolism, since it catalyzes the conversion of H_2O_2 to H_2O in the ascorbate-glutathione cycle⁴². Compared with the activity of APX, the protein and gene level showed a significant decrease at the CN (Fig. 5F,G), indicating that the antioxidative system was inhibited at the CN. These results were consistent with previous findings in the aged seed of soybean, maize, and other species^{11–13}. The decreased capacity of the antioxidative system could lead to ROS accumulation, reflecting the oxidative damage and increased protein carbonylation.

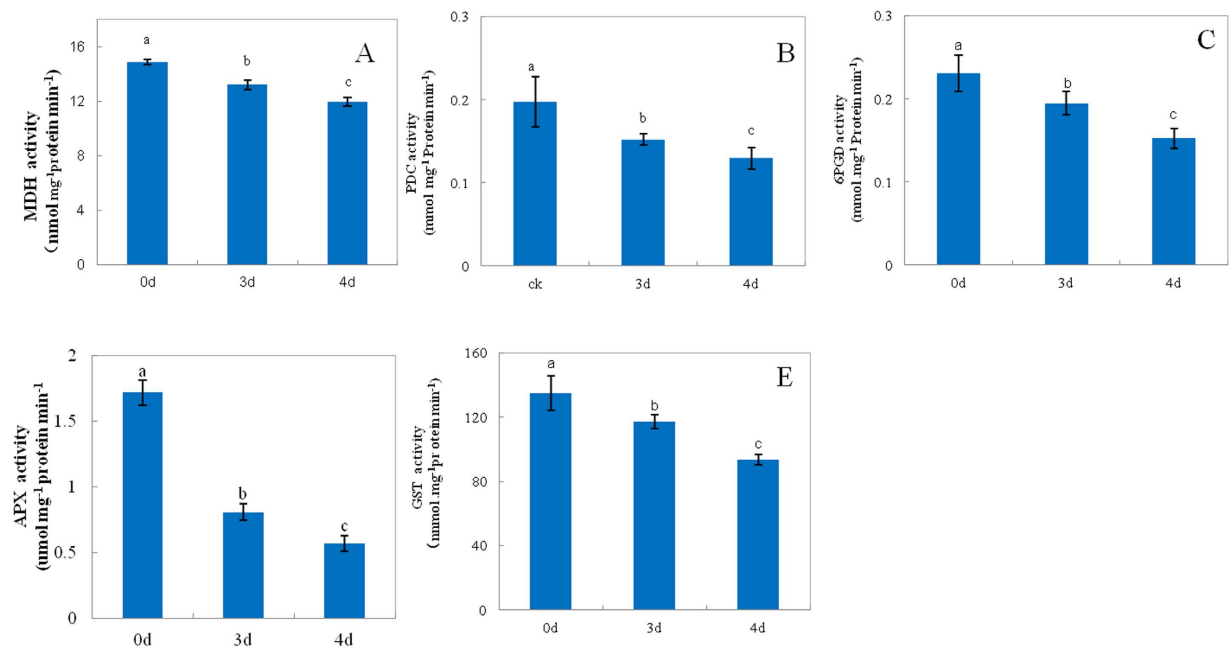
GST catalyzes the conjugation of the reduced form of glutathione to xenobiotic substrates for the purpose of detoxification⁴³ and protects against oxidative damage by ROS⁴⁴. In the present study, the activity of GST showed

Spot	Protein name	Accession No.	Scores
Down-regulation			
Energy			
C42	Vacuolar ATPase B subunit	NP_001057902.1	316
C46	Phosphoglycerate kinase	ABI74567.1	899
C47	Glucose and ribitol dehydrogenase homolog	Q75KH3.2	664
Transcription			
C45	Eukaryotic initiation factor 4A-1	BAA02152.1	448
C48	Elongation factor Tu	NP_001051912.1	415
Metabolism			
C50	Aconitate hydratase, cytoplasmic	Q6YZX6.1	671
C51	Pyruvate kinase 1, cytosolic	NP_001065749.1	194
Disease and defense			
C41	60 kDa chaperonin alpha subunit	AAP44754.1	215
Secondary metabolism			
C44	Lactoylglutathione lyase	BAB71741.1	797
Growth/division			
C43	Actin-1	NP_001051086.1	573
Protein destination and storage			
C49	T complex protein	NP_001057876.1	227
Up-regulation			
Protein destination and storage			
C52	19 kDa globulin	CAA45400.1	161
C53	Cupin family protein	AAS07324.1	155
C56	Glutelin type-A 3	CAA38211.1	342
C57	Glutelin type-A 1	AAA33906.1	228
C58	Glutelin type-A 2	BAA00462.1	315
C60	Glutelin type-B 5	BAC77349.1	280
C67	Cupin family protein	AAS07324.1	575
Metabolism			
C55	Proteasome subunit alpha type-6	NP_001049162.1	133
C59	Glyceraldehyde-3-phosphate dehydrogenase 2, cytosolic	NP_001053139.1	344
Energy			
C61	Formate dehydrogenase 1, mitochondrial	BAA77337.1	295
C65	Pyrophosphate-dependent phosphofructokinase alpha subunit	NP_001061602.1	263
C66	Glucose-6-phosphate isomerase, cytosolic A	BAA08148.1	178
C68	ATP synthase subunit c, chloroplastic	CAA48649.1	179
Unclear classification			
C54	Os05g0569500 protein	NP_001056364.1	361

Table 3. Proteins with no significantly changed abundance and significant carbonylation at the critical node in 0-d, 3-d, and 4-d aged rice seeds. Mascot scores >65 are statistically significant at $p < 0.05$.

significant decrease at the CN (Fig. 4E), indicating that rice seed was affected by ROS. Additionally, we observed the specific carbonylation of proteins related to oxidative stress such as HSPs and chaperonins. HSPs are encoded by multigene families⁴⁵; small HSP class I (17.9 kDa) belongs to the small HSP family, which is expressed in rice seed^{45,46}. HSPs and chaperonins play an important role in protein folding and protect cells against stress⁴⁷. Carbonylated HSPs and chaperonins were described in aged *Arabidopsis* seeds²². The downregulation of HSPs and chaperonins disrupted the defense system and might cause oxidative damage at the CN.

Our study revealed the carbonylation of upregulated proteins, such as SSP, at the CN. Previous studies reported that the degradation of storage proteins is associated with seed viability⁴⁸ and that the seed of SSP mutants is sensitive to ageing²². In the present study, SSP displayed a significant upregulation and various experimental molecular weights at the CN (Figs 2B and 3). Our results suggest that the seed had a decreased ability to utilize SSPs at the CN, which might cause SSP accumulation and carbonylation. Previous studies reported that SSP might be a primary target for oxidative stress and protect other proteins for oxidative damage during seed ageing^{22,49}. Our results suggest that the increased carbonylation level of SSP indicates the relatively high ROS levels at the CN. Our results were consistent with the decreased capacity of the antioxidant system at the CN.



Ageing treatment

Figure 4. The activity of malate dehydrogenase (MDH, (A)) pyruvate decarboxylase (PDC, (B)) 6-phosphogluconate dehydrogenase (6PGD, (C)) ascorbate peroxidase (APX, (D)) and glutathione S-transferase (GST, (E)) in 0-d, 3-d, and 4-d aged rice seeds after imbibition for 48 h. Data represent the mean \pm standard deviation of three independent experiments. All treatments significantly differed from the control at $p < 0.05$ ($n = 3$).

Conclusion

This study revealed that oxidative stress was related to the loss of seed viability. Our findings indicated the effects of oxidative stress at the CN, since the proteins related to energy and defense metabolism were downregulated and/or inactivated. The ability to utilize SSPs was also reduced, leading to a rapid decline in seed viability at the P-II.

Materials and Methods

Plant material and treatments. Rice seed (*Oryza sativa* L. *japonica nipponbare*) was obtained from the Jiangxi Agricultural Academy of Sciences, Nanchang, China. Rice seeds were treated at 40 °C and 75% relative humidity for 0 d, 3 d, and 4 d to decrease the germination rate by 3%, 8%, and 16%, respectively¹. The embryos were extracted after seed imbibition at 28 °C for 48 h in the dark, and then stored at -80 °C until analysis.

Proteomic and carbonylation analysis. The frozen embryos were ground with a mortar and pestle using a buffer, containing 0.1 M Tris-HCl (pH 7.5), 0.1% dithiothreitol (DTT), 2% polyvinylpyrrolidone (PVPP), and 0.5% ethylenediaminetetraacetic acid (EDTA). Protein was extracted using the Tris-phenol protocol⁵⁰, and then, 500 μ g of protein was applied to rehydrated gel strips with an immobilized linear pH gradient of 5–8 (BioRad, Hercules, CA, USA). The first-dimensional IEF was performed at 20 °C on a flat-bed electrophoresis unit (BioRad) as follows: rehydration for 12 h, 0 V to 150 V in 15 min, 150 V to 1,000 V in 1 h, 1,000 V to 8,000 V in 5 h, and 8,000 V until a total of 60 kVh. After IEF, the strips were: 1) equilibrated for 15 min in Solution A, containing 6 M urea, 20% (v/v) glycerol, 2% (w/v) SDS, 375 mM Tris-HCl (pH 8.8), and 2% (w/v) DTT, and then, in Solution B, containing 6 M urea, 20% (v/v) glycerol, 2% (w/v) SDS, 375 mM Tris-HCl (pH 8.8), and 2.5% iodoacetamide for analyzing the proteomic profile and 2) derivatized by incubating in 10 mM DNPH for 20 min with gentle agitation, and then, equilibrated as described above for analyzing the profile of carbonylated proteins. The equilibrated strips were placed on SDS-PAGE using homogenous 12% (v/v) polyacrylamide gels with 4% (v/v) stacking gels (BioRad). Gel electrophoresis was performed at 250 V with circulating cooling using a running buffer, containing 25 mM Tris (pH 8.3), 195 mM glycine, and 0.1% (w/v) SDS. The gels were stained with CBB G250 or transferred to PVDF membrane and detected with anti-DNP antibodies. Gel images were obtained using a flatbed scanner and analyzed by PDQuest 5.0 (BioRad). Spot intensity was calculated according to the relative expression volume. Spots with a fold change higher than 1.5 were excised for mass spectrometry.

In-gel digestion, mass spectrometry, and database searching. The protein and carbonylated protein that were corresponded the protein spot on 2D gels, were excised into 1-mm³ pieces from 2D gels and de-stained with 25 mM NH₄CO₃ in 50% acetonitrile. The gels were dehydrated by adding acetonitrile and then, digested with 25 μ l of 0.1 mM trypsin in 25 mM NH₄CO₃ for 15 min⁵¹. The excess trypsin solution was removed, and gel pieces were incubated at 37 °C overnight in 20 μ l of 25 mM NH₄CO₃. A mixture of 1 μ l peptide solution

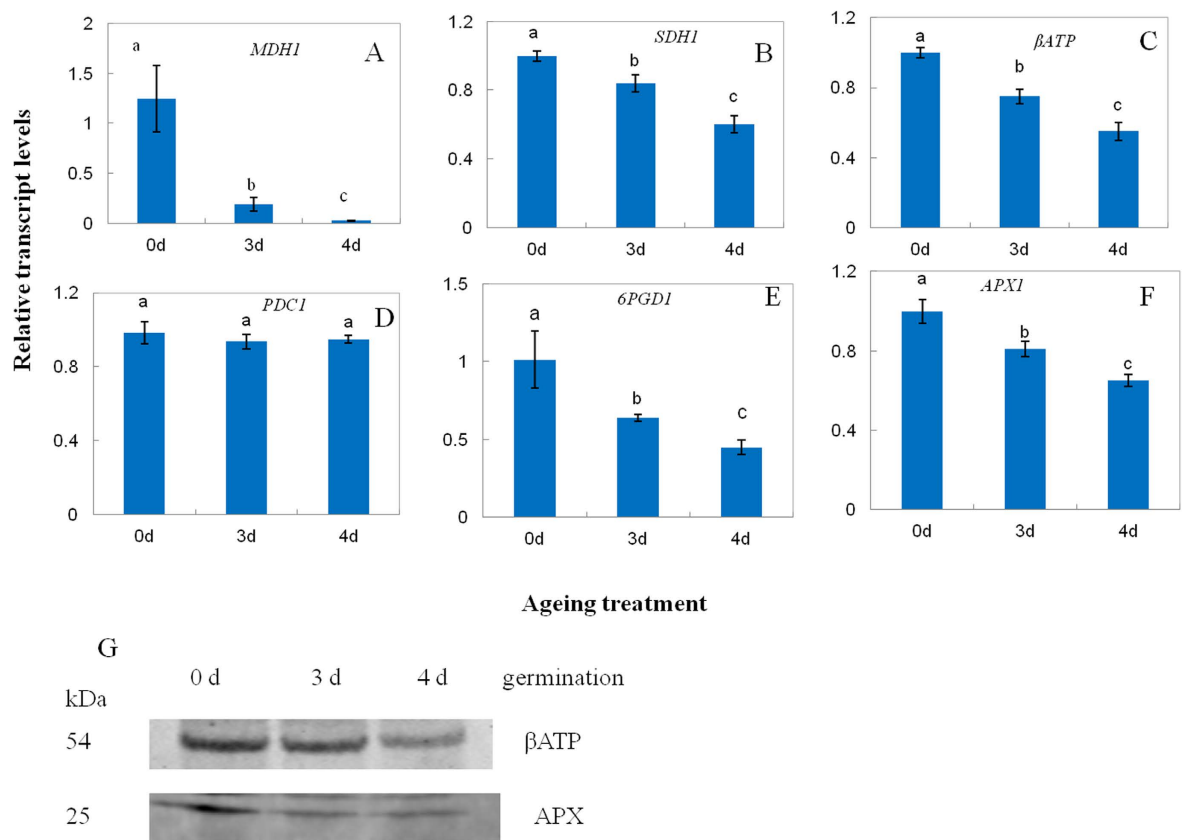


Figure 5. Relative levels of malate dehydrogenase 1 (*MDH1*, (A)) succinate dehydrogenase 1 (*SDH1*, (B)) β ATP synthase (C) pyruvate decarboxylase 1 (*PDC1*, (D)) 6-phosphogluconate dehydrogenase 1 (*6PGD1*, (E)) and ascorbate peroxidase 1 (*APXI*, (F)) and abundance of beta subunit of ATP synthase (βATP) and ascorbate peroxidase (APX) (G) in 0-d, 3-d, and 4-d aged rice seeds after imbibition for 48 h. Transcript levels in 3-d and 4-d aged seeds were calculated in relation to a value of 1.0 that assigned to 0-d aged seeds after imbibition for 48 h. Data represent the mean ± standard deviation of three independent experiments. All treatments significantly differed from the control at $p < 0.05$ ($n = 3$).

and 1 μl matrix solution with 1 mg ml⁻¹, a-cyano-4-hydroxycinnamic acid in 70% acetonitrile, and 0.1% trifluoroacetic acid was loaded onto the AnchorChip MALDI target plate (Bruker Daltonics, Manning Park Billerica, MA, USA) and analyzed by a matrix assisted laser desorption-ionization time of flight (MALDI-TOF)/TOF mass spectrometer (Bruker Daltonics), according to the manufacturer's instructions. MS data were uploaded to the Mascot server using Biotoools (Bruker Daltonics) and searched against the National Center for Biotechnology Information (NCBI) protein database (25,010,123 sequences; 8,625,376,125 residues; search parameters, rice; proteolytic enzyme, trypsin; maximum missed cleavages, 1; fix modifications, carbamidomethyl; variable modifications, oxidation; peptide mass tolerance, 100 ppm; fragment mass tolerance, 0.5 Da). Spots with a Mowse score higher than 65 were considered as proteins.

Assay of enzyme activities. The activity of MDH was determined at 340 nm as described by Glatthaar *et al.*⁵². The activity of PDC was measured in a reaction medium, containing 200 mM Tris-HCl (pH 6.0), 100 mM pyruvate, 0.1 mM thiamine pyrophosphate, 1.0 mM MgCl₂, 9.0 units of alcohol dehydrogenase, and 225 μM NADH as described⁵³ with minor modifications. The activity of APX was determined at 290 nm as described by Nakano and Asada⁵⁴. The activity of GST was determined at 340 nm as described by Habig *et al.*⁵⁵. The activity of 6PGD was determined in 50 mM Tris-HCl (pH 7.5) and 0.25 mM NADP, started with 2 mM 6-phosphogluconate as described by Bailey-Serres and Nguyen⁵⁶.

Immunoblot analysis. Equal amounts of rice embryo proteins (10 μg per lane) were loaded onto SDS-PAGE gels, transferred to PVDF, and incubated with βATP and APX antibodies. Anti-rabbit IgG was used as a secondary antibody (Agrisera, Vannas, Sweden). Immunodetection was performed using the Chemiluminescent Substrate Kit (KPL, Hemet, CA, USA).

Quantitative real-time polymerase chain reaction (qRT-PCR). Total RNA was isolated from rice embryos after seed imbibition for 48 h using the RNeasy pure plant kit (Qiagen, Beijing, China). Specific primer pairs (Supplemental Table 1) were designed using Primer 5 (Premier Biosoft, Palo Alto, CA, USA). qRT-PCR was

performed using the Roche LightCycler® 480II. The thermal cycling program was as follows^{57,58}: 95 °C for 15 min, 40 cycles at 95 °C for 15 s and at 60 °C for 30 s. The gene expression of rice *UBQ5* was used as an internal control.

Protein concentration assay. Protein concentration was determined as described by Bradford⁵⁹ using bovine serum albumin as a standard.

Statistical analysis. Data were pooled across repeated experiments. Analysis of variance in conjunction with the least significant difference test was performed by SPSS (IBM, Chicago, IL, USA). Differences were considered significant at $p < 0.05$.

References

1. Yin, G. K. *et al.* Comprehensive mitochondrial metabolic shift during the critical node of seed ageing in Rice. *PLoS One*. **11**, e0148013 (2016).
2. Walters, C., Wheeler, L. M. & Stanwood, P. C. Longevity of cryogenically stored seeds. *Cryobiology* **48**, 229–244 (2004).
3. FAO. Second report on the state of the world's plants genetic resources for food and agriculture. Commission on Genetic Resources for Food and Agriculture, Food and Agriculture Organization of The United Nations, Rome, pp. 47 (2010).
4. Börner, A., Chebotar, S. & Korzun, V. Molecular characterization of the genetic integrity of wheat (*Triticum aestivum* L.) germplasm after long-term maintenance. *Theor. Appl. Genet.* **100**, 494–497 (2000).
5. Hay, F. R. *et al.* Viability of *Oryza sativa* L. seeds stored under genebank conditions for up to 30 years. *Genet. Resour. Crop Ev.* **60**, 275–296 (2013).
6. Hay, F. R., de Guzman, F. & Sackville Hamilton, N. R. Viability monitoring intervals for genebank samples of *Oryza sativa*. *Seed Sci. Technol.* **43**, 218–237 (2015).
7. Hintum, T. J., van De Wiel, C. C. M., Visser, D. L., Van Treuren, R. & Vosman, B. The distribution of genetic diversity in a *Brassica oleracea* gene bank collection related to the effects on diversity of regeneration, as measured with AFLPs. *Theor. Appl. Genet.* **114**, 777–786 (2007).
8. FAO. Genbank Standards 2014. Food and Agriculture Organization of The United Nations, Rome, 36 (2014).
9. Bailly, C. & Kranner, I. Analyses of reactive oxygen species and antioxidants in relation to seed longevity and germination. In *Seed Dormancy*. Humana Press. (pp. 343–367) (2011).
10. Rajjou, L. & Debeaujon, I. Seed longevity: survival and maintenance of high germination ability of dry seeds. *C. R. Biol.* **331**, 796–805 (2008).
11. Xin, X. *et al.* Proteome analysis of maize seeds: the effect of artificial ageing. *Physiol. Plantarum* **143**, 126–138 (2011).
12. Yin, G. K. *et al.* Activity levels and expression of antioxidant enzymes in the ascorbate–glutathione cycle in artificially aged rice seed. *Plant Physiol. Biochem.* **80**, 1–9 (2014).
13. Xin, X. *et al.* Reduced mitochondrial and ascorbate–glutathione activity after artificial ageing in soybean seed. *J. Plant Physiol.* **171**, 140–147 (2014).
14. Wang, Y., Li, Y., Xue, H., Pritchard, H. W. & Wang, X. Reactive oxygen species-provoked mitochondria-dependent cell death during ageing of elm (*Ulmus pumila* L.) seeds. *Plant J.* **81**, 438–452 (2015).
15. Petla, B. P. *et al.* Rice PROTEIN I-ISOASPARTYL METHYLTRANSFERASE isoforms differentially accumulate during seed maturation to restrict deleterious isoAsp and reactive oxygen species accumulation and are implicated in seed vigor and longevity. *New Phytol.* **211**, 627–645 (2016).
16. Wong, C. M., Marcocci, L., Liu, L. & Suzuki, Y. J. Cell signaling by protein carbonylation and decarbonylation. *Antioxid. Redox Signal.* **12**, 393–404 (2010).
17. Ramallo Guevara, C. *et al.* Global protein oxidation profiling suggests efficient mitochondrial proteome homeostasis during ageing. *Mol. Cell. Proteomics*. mcp.M115.055616 (2016).
18. Qin, G. Z., Wang, Q., Liu, J., Li, B. Q. & Tian, S. P. Proteomic analysis of changes in mitochondrial protein expression during fruit senescence. *Proteomics* **9**, 4241–4253 (2009).
19. Havé, M., Leita, L., Bagard, M., Castell, J. F. & Repellin, A. Protein carbonylation during natural leaf senescence in winter wheat, as probed by fluorescein-5-thiosemicarbazide. *Plant Biol.* **17**, 973–979 (2015).
20. Zhang, H. *et al.* Analysis of dynamic protein carbonylation in rice embryo during germination through AP-SWATH. *Proteomics*. pmic.201500248 (2016).
21. Rajjou, L. *et al.* Proteome-wide characterization of seed aging in *Arabidopsis*. A comparison between artificial and natural aging protocols. *Plant Physiol.* **148**, 620–641 (2008).
22. Nguyen, T. P., Cueff, G., Hegedus, D. D., Rajjou, L. & Bentsink, L. A role for seed storage proteins in *Arabidopsis* seed longevity. *J. Exp. Bot.* **66**, 6399–6413 (2015).
23. Yin, X., He, D., Gupta, R. & Yang, P. Physiological and proteomic analyses on artificially aged *Brassica napus* seed. *Front Plant Sci.* **6**, fppls.2015.00112 (2015).
24. Bevan, M. *et al.* Analysis of 1.9 Mb of contiguous sequence from chromosome 4 of *Arabidopsis thaliana*. *Nature* **391**, 485–488 (1998).
25. Stadtman, E. R. Role of oxidant species in aging. *Curr. Med. Chem.* **11**, 1105–1112 (2004).
26. Møller, I. M., Jensen, P. E. & Hansson, A. Oxidative modifications to cellular components in plants. *Annu. Rev. Plant Biol.* **58**, 459–481 (2007).
27. Bewley, J. D. Seed germination and dormancy. *Plant Cell* **9**, 1055–1066 (1997).
28. Narsai, R., Law, S. R., Carrie, C., Xu, L. & Whelan, J. In-depth temporal transcriptome profiling reveals a crucial developmental switch with roles for RNA processing and organelle metabolism that are essential for germination in *Arabidopsis*. *Plant Physiol.* **157**, 1342–1362 (2011).
29. Law, S. R. *et al.* Nucleotide and RNA metabolism prime translational initiation in the earliest events of mitochondrial biogenesis during *Arabidopsis* germination. *Plant Physiol.* **158**, 1610–1627 (2012).
30. Sweetlove, L. J. *et al.* The impact of oxidative stress on *Arabidopsis* mitochondria. *Plant J.* **32**, 891–904 (2002).
31. Sew, Y. S., Ströher, E., Fenske, R. & Millar, A. H. Loss of mitochondrial malate dehydrogenase activity alters seed metabolism impairing seed maturation and post-germination growth in *Arabidopsis*. *Plant Physiol.* **171**, 849–863 (2016).
32. Huang, S. & Millar, A. H. Sequence diversity and conservation in factors influencing succinate dehydrogenase flavinylation. *Plant Signal Behav.* **8**, e22815 (2013).
33. Gleason, C. *et al.* Mitochondrial complex II has a key role in mitochondrial-derived reactive oxygen species influence on plant stress gene regulation and defense. *Proc. Natl. Acad. Sci. USA*. **108**, 10768–73 (2011).
34. Zhao, Z. & Assmann, S. M. The glycolytic enzyme, phosphoglycerate mutase, has critical roles in stomatal movement, vegetative growth, and pollen production in *Arabidopsis thaliana*. *J. Exp. Bot.* **62**, 5179–5189 (2011).
35. Agarwal, S., Kapoor, A., Lakshmi, O. S. & Grover, A. Production and phenotypic analysis of rice transgenics with altered levels of pyruvate decarboxylase and alcohol dehydrogenase proteins. *Plant Physiol. Biochem.* **45**, 637–646 (2007).

36. Sharma, S., Mustafiz, A., Singla-Pareek, S. L., Shankar Srivastava, P. & Sopory, S. K. Characterization of stress and methylglyoxal inducible triose phosphate isomerase (OscTPI) from rice. *Plant Signal. Behav.* **7**, 1337–1345 (2012).
37. Fukayama, H. *et al.* Characterization and expression analyses of two plastidic enolase genes in rice. *Biosci. Biotechnol. Biochem.* **79**, 402–409 (2015).
38. Rye, P. T. & Lamarr, W. A. Measurement of glycolysis reactants by high-throughput solid phase extraction with tandem mass spectrometry: Characterization of pyrophosphate-dependent phosphofructokinase as a case study. *Anal. Biochem.* **482**, 40–47 (2015).
39. Pinhero, R. G. *et al.* Alleviation of low temperature sweetening in potato by expressing Arabidopsis pyruvate decarboxylase gene and stress-inducible rd29A: A preliminary study. *Physiol. Mol. Biol. Plants.* **17**, 105–114 (2011).
40. Mithran, M., Paparelli, E., Novi, G., Perata, P. & Loreti, E. Analysis of the role of the pyruvate decarboxylase gene family in Arabidopsis thaliana under low-oxygen conditions. *Plant Biol.* **16**, 28–34 (2014).
41. Fernández-Fernández, Á. D. & Corpas, F. J. *In Silico* Analysis of Arabidopsis thaliana Peroxisomal 6-Phosphogluconate Dehydrogenase. *Scientifica (Cairo)*. 3482760 (2016).
42. Teixeira, F. K., Menezes-Benzvente, L., Galvão-Margis, V. C. R. & Margis-Pinheiro, M. Rice ascorbate peroxidase gene family encodes functionally diverse isoforms localized in different subcellular compartments. *Planta* **224**, 300–314 (2006).
43. Hayes, J. D. & McLellan, L. Glutathione and glutathione-dependent enzymes represent a co-ordinately regulated defence against oxidative stress. *Free Radic. Res.* **31**, 273–300 (1999).
44. Moons, A. Regulatory and functional interactions of plant growth regulators and plant glutathione S-transferases (GSTs). *Vitam. Horm.* **72**, 155–202 (2005).
45. Sarkar, N. K., Kim, Y. K. & Grover, A. Rice sHsp genes: genomic organization and expression profiling under stress and development. *BMC Genomics* **10**, 393 (2009).
46. Zimmermann, P. *et al.* Genevestigator transcriptome meta-analysis and biomarker search using rice and barley gene expression databases. *Mol. Plant.* **1**, 851–857 (2008).
47. Morano, K. A. New tricks for an old dog: the evolving world of Hsp70. *Ann. N. Y. Acad. Sci.* **1113**, 1–14 (2007).
48. Müntz, K., Belozersky, M. A., Dunaevsky, Y. E., Schlereth, A. & Tiedemann, J. Stored proteinases and the initiation of storage protein mobilization in seeds during germination and seedling growth. *J. Exp. Bot.* **52**, 1741–52 (2001).
49. Davies, M. J. The oxidative environment and protein damage. *Biochim. Biophys. Acta.* **1703**, 93–109 (2005).
50. Islam, N., Lonsdale, M., Upadhyaya, N. M., Higgins, T. J., Hirano, H. & Akhurst, R. Protein extraction from mature rice leaves for two-dimensional gel electrophoresis and its application in proteome analysis. *Proteomics* **4**, 1903–1908 (2004).
51. Liu, B., Qin, F., Liu, W. & Wang, X. Differential proteomics profiling of the ova between healthy and *Rice stripe virus*-infected female insects of *Laodelphax striatellus*. *Sci Rep.* **6**, 27216 (2016).
52. Glatthaar, B. E., Barbarash, G. R., Noyes, B. E., Banaszak, L. J. & Bradshaw, R. A. The preparation of the cytoplasmic and mitochondrial forms of malate dehydrogenase and aspartate aminotransferase from pig heart by a single procedure. *Anal. Biochem.* **57**, 432–451 (1974).
53. Conway, T., Osman, Y. A., Konnan, J. I., Hoffmann, E. M. & Ingram, L. O. Promoter and nucleotide sequences of the *Zymomonas mobilis* pyruvate decarboxylase. *J. Bacteriol.* **169**, 949–954 (1987).
54. Nakano, Y. & Asada, K. Hydrogen peroxide is scavenged by ascorbate-specific peroxidase in spinach chloroplasts. *Plant Cell Physiol.* **22**, 867–880 (1981).
55. Habig, W. H., Pabst, M. J. & Jakoby, W. B. Glutathione S transferases-The first enzymatic step in mercapturic acid formation. *J. Biol. Chem.* **249**, 7130–7139 (1974).
56. Bailey-Serres, J. & Nguyen, M. T. Purification and characterization of cytosolic 6-phosphogluconate dehydrogenase isozymes from maize. *Plant Physiol.* **100**, 1580–1583 (1992).
57. Than, W., Qin, F., Liu, W. & Wang, X. Analysis of *Sogatella furcifera* proteome that interact with P10 protein of *Southern rice black-streaked dwarf virus*. *Sci Rep.* **6**, 32445 (2016).
58. Liu, W., Gray, S., Huo, Y., Li, L., Wei, T. & Wang, X. Proteomic Analysis of Interaction between a Plant Virus and Its Vector Insect Reveals New Functions of Hemipteran Cuticular Protein. *Mol Cell Proteomics.* **14**, 2229–2242 (2015).
59. Bradford, M. M. A rapid and sensitive method for the quantitation of microgram quantities of protein utilizing the principle of protein-dye binding. *Ann. Biochem.* **72**, 248–254 (1976).

Acknowledgements

This work was supported by the National Natural Science Foundation of China Program (31371713 and 31401470), the National Key Technology R&D Program (2013BAD01B01), the Agricultural Science and Technology Innovation Program/Crop Germplasm Resources Preservation and Sharing Innovation Team. JW is supported by grants from the Australian Research Council (CE140100008).

Author Contributions

G.Y., X.L. and J.W. designed the research. G.Y., S.F., M.A. and S.W. performed experiments, G.Y., X.X., X.C., J.Z. and J.H. analysed the results. G.Y. and J.W. wrote the paper, X.X., X.C., J.Z. and J.H. helped with editing the paper before submission. All authors reviewed the manuscript.

Additional Information

Supplementary information accompanies this paper at <http://www.nature.com/srep>

Competing financial interests: The authors declare no competing financial interests.

How to cite this article: Yin, G. *et al.* Proteomic and Carbonylation Profile Analysis at the Critical Node of Seed Ageing in *Oryza sativa*. *Sci. Rep.* **7**, 40611; doi: 10.1038/srep40611 (2017).

Publisher's note: Springer Nature remains neutral with regard to jurisdictional claims in published maps and institutional affiliations.



This work is licensed under a Creative Commons Attribution 4.0 International License. The images or other third party material in this article are included in the article's Creative Commons license, unless indicated otherwise in the credit line; if the material is not included under the Creative Commons license, users will need to obtain permission from the license holder to reproduce the material. To view a copy of this license, visit <http://creativecommons.org/licenses/by/4.0/>

© The Author(s) 2017